Idaho State University

Post-Fire Vegetation Regrowth Analysis Using Free and Open-Source Software and Data

Christina Appleby

GEOL 6628: Advanced GIS Programming

Professor Wu

May 5, 2023

Abstract

This study on post-fire vegetation regrowth in the Cold Fire burn scar in California utilized free and open-source software (FOSS) and data, including various Python packages, Jupyter notebook, QGIS, and earth observation data. The use of these tools provided several advantages, including cost-effectiveness and the ability to customize and modify the analysis. By utilizing pre- and post-fire Normalized Difference Vegetation Index (NDVI) data and employing linear regression analysis, this study assessed the impact of slope, aspect, and burn severity on post-fire vegetation regrowth in the Cold Fire burn scar in California. The findings showed that the burned area demonstrated a moderate recovery to pre-fire conditions, with regrowth rates being most significant in the second and third years following the fire. Furthermore, the study revealed that regrowth was higher on steeper and south-facing slopes, as well as areas with lower burn severity. It also proved that FOSS for GIS is effective for accessing post-fire vegetation regrowth. The code for this study can be found on GitHub.

1. Introduction

Post-fire vegetation regrowth analyses are crucial for land management because they offer valuable insights into the ecosystem's recovery following a wildfire (Mitri & Gitas, 2013). These analyses enable land managers to identify areas that are more or less resilient to fire and anticipate potential risks, such as increased erosion, invasive species, or vegetation type conversion (Arianoutsou et al., 2011; Guiterman et al., 2022; Wittenberg, 2021). By utilizing this information, land managers can make informed decisions about managing the land after a fire, including whether to actively promote recovery or allow natural regeneration to occur. Additionally, these analyses can aid in prioritizing management efforts and targeting resources to

areas that require restoration, thereby preventing further damage to the ecosystem and ensuring sustainable and resilient land management practices (*After Fire: Toolkit for the Southwest*, n.d.).

Hypotheses

The vegetation regrowth hypotheses were as follows:

1. Areas with higher burn severity will have slower regrowth than areas with lower burn severity based on the study area for this analysis being approximately 40 kilometers from the Crotteau et al. (2013) study area.
2. North-facing slopes will have higher regrowth than south-facing slopes.
3. Steeper slopes will have lower regrowth than milder slopes.
4. Regrowth rates will be higher in the first few years following the fire (Meng et al., 2015; Bright et al., 2019).

Study Area

On June 21, 2008, the Cold Fire was ignited by a lightning strike and burned an estimated 5,600 acres of land (Figure 1). The majority of the study area was characterized by verdant vegetation, mainly comprising evergreen forests. Prior to 2008, the fire perimeter had experienced three fires, with two of them occurring over 30 years ago, and one of them happening less than 20 years prior and affecting an area of less than 20 acres. In 2020, the Dixie Fire only impacted the northern edge of the Cold Fire burn scar.

The study area has an elevation ranging from roughly 4,100 to 7,000 feet above sea level. Based on the Environmental Protection Agency's ecoregion research (2022), the region is predominantly covered by a combination of coniferous trees, such as white fir, Douglas-fir, and Jeffery pine, among others. The soil moisture regime is classified as mostly xeric, which

indicates that the area experiences cool and moist winters and warm and dry summers (*Ecoregions | US EPA*, 2022). Typically, summer temperatures do not exceed 90˚F, while winter temperatures can drop down to around 26˚F. The average annual precipitation is approximately 45 inches, with most of the rainfall occurring between December and March (NOAA's National Weather Service, n.d.).

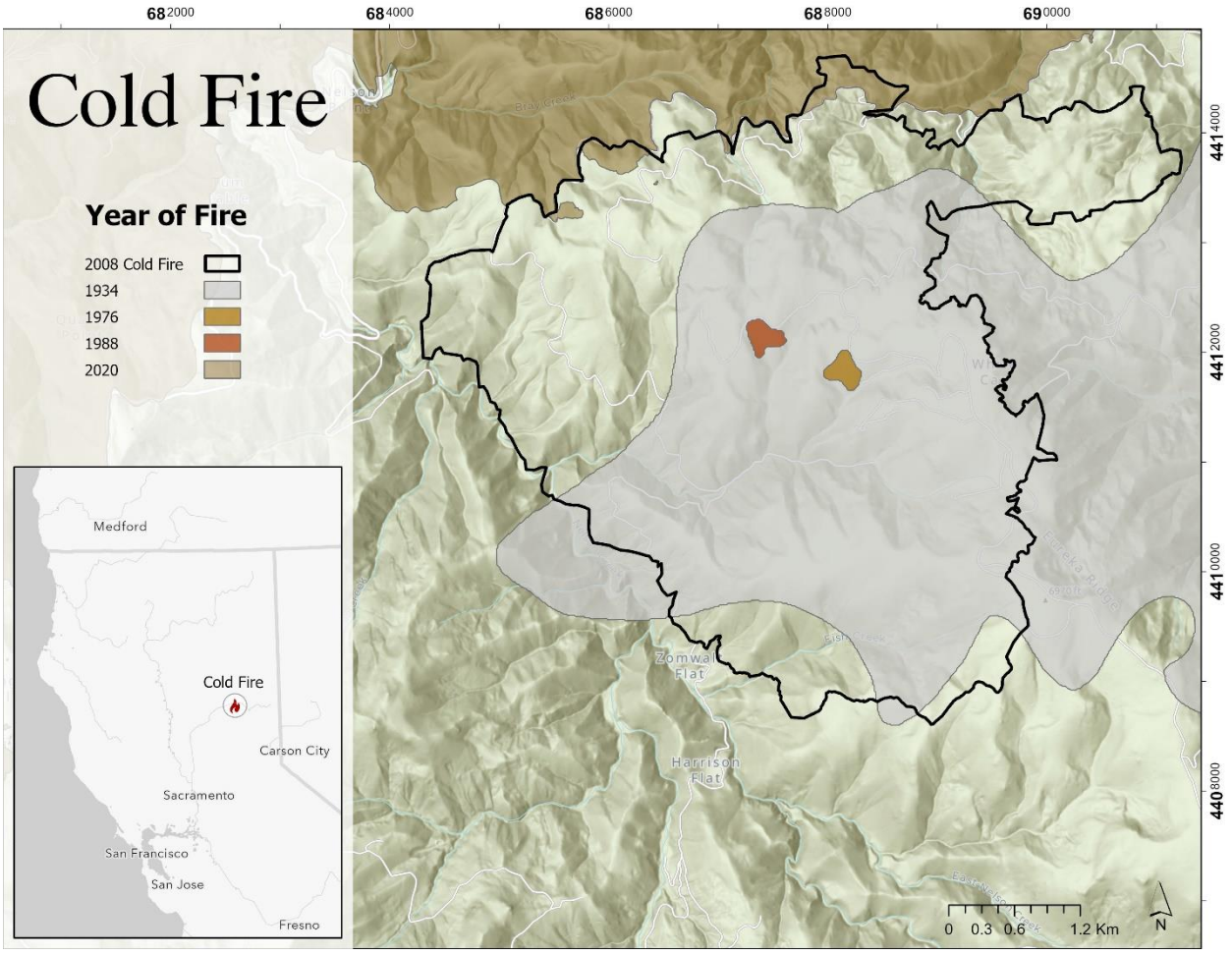

Figure 1 - Map of the Cold Fire and intersecting fire perimeters.

Free and Open-Source Software

Proprietary GIS software is generally easier to use than FOSS (Maurya et al., 2015), but the licenses can cost a premium. FOSS for GIS allows those who cannot afford proprietary software to incorporate GIS into their work or studies (Flenniken et al., 2020), and it fosters innovation because new software products can be built upon the work of others (Coetzee et al., 2020). Additional advantages of FOSS for GIS include community support, scalability without increased costs, open data formats that are easy to port, and the ability to experiment with new software without a trial time limit or paying the full licensing fee (Maurya et al., 2015). A disadvantage of FOSS for GIS is that it requires more effort to use. There are numerous open-source projects available, and not only are some not maintained, but it takes time to find the best one for your application. Additionally, many open-source projects lack a graphical user interface (GUI), and those that do have a GUI are not always intuitive (Maurya et al., 2015).

Although FOSS for GIS has been around since the 1980s, it wasn't until 2006 that the not-for-profit Open Source Geospatial Foundation (OSGeo) was created (Coetzee et al., 2020) with a mission "to support the collaborative development of open source geospatial software, and promote its widespread use" (*OSGeo Description - OSGeo*, n.d.). Popular OSGeo projects are the Geospatial Data Abstractions Library (GDAL), PostGIS spatial database, and Quantum GIS (QGIS) desktop software, among others. Popular non-OSGeo products include various geospatial libraries in the R data science language and the Python programming language, and OpenDroneMap for processing and analyzing drone imagery.

A substantial portion of studies do not include information on the software used, whether proprietary or FOSS (Muenchow et al., 2019). Of the seven post-fire vegetation regrowth and

recovery papers reviewed for this study (Bright et al., 2019; Casady et al., 2010; Meng et al., 2015; Petropoulos et al., 2014; Strand et al., 2019; Tonbul et al., 2016; Viana-Soto et al., 2017), only one mentioned the software used for their analysis. Of the four papers reviewed related to using FOSS for GIS (Duarte et al., 2019; Knevels et al., 2019; Mangiameli et al., 2021; Mattivi et al., 2019), only one identified exactly where to find their code. Sharing the resources used for research, such as software used, code, and data, can assist others in reproducing, replicating, or even building upon that research.

The goal of this study was not only to analyze post-fire vegetation regrowth, but to also use only FOSS for GIS, specifically geospatial Python libraries, and to share all the code used in the study. An effort was also made to add comments to the code and Jupyter Notebook for better understanding.

2. Data and Methodology

Factors Affecting Post-Fire Vegetation Regrowth

There are numerous factors that affect post-fire vegetation regrowth, and not all are covered or used in this study. A very important factor is climate, and various metrics affect post-fire regrowth differently. As to be expected, drought (Savage et al., 2013) and drought severity (Harvey et al., 2016) have a negative effect, and longer growing seasons (Urza & Sibold, 2017) and increased precipitation (Welch et al., 2016) have a positive effect. However, climate metrics were not included in this analysis.

Burn Severity

Burn severity pertains to the magnitude of organic matter loss, both above and below the ground, due to a fire. Burn severity and fire severity are frequently used interchangeably. After a fire has occurred, burn severity is frequently used in Burned Area Emergency Response (BAER) assessments to measure the degree of change brought about by the fire (Keeley, 2009).

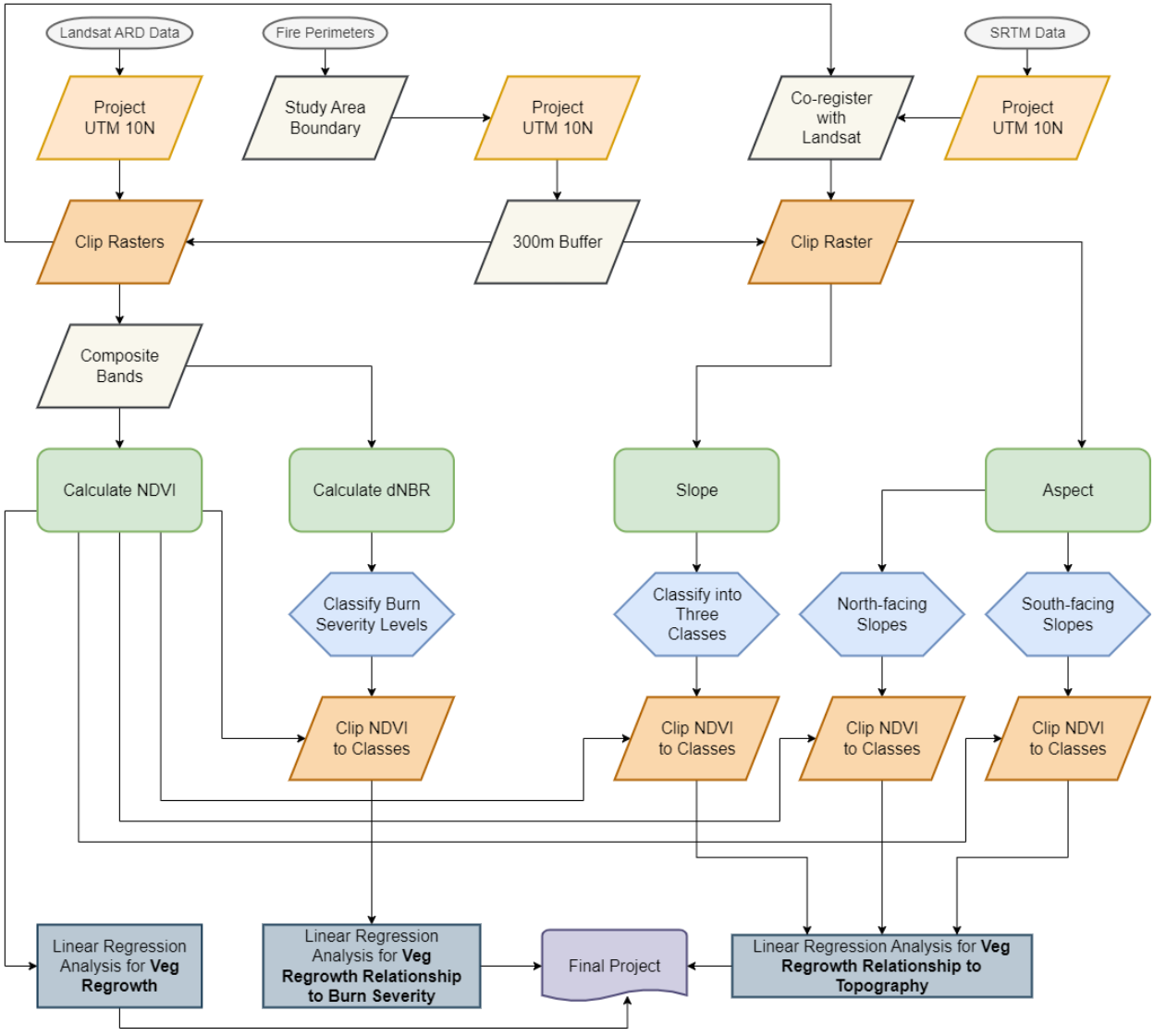

Figure 2 - Workflow used for post-fire vegetation regrowth analysis.

According to Crotteau et al. (2013), areas with high severity burns typically have fewer seedling densities and a greater distance from seed sources, leading to reduced tree regeneration compared to low or moderate severity burned regions. Nonetheless, Johnstone and Chapin (2006) discovered that high severity burns may provide seeds with better access to mineral soils as they burn through the upper organic layer. Additionally, certain pine tree species have serotinous cones that only release seeds when heated by a wildfire (Johnson & Gutsell, 1993).

The differenced Normalized Burn Ratio (dNBR) is a commonly used spectral index to assess burn severity, which is calculated using the near infrared (NIR) and shortwave infrared (SWIR) spectral bands. The NIR band is a reliable indicator of plant health as healthy vegetation with more chlorophyll reflects more NIR energy, as opposed to vegetation that is unhealthy (*Reflected Near-Infrared Waves | Science Mission Directorate*, n.d.). Conversely, the SWIR band is more effective at detecting soil and vegetation with lower water content (Holzman et al., 2021). After a fire, NIR reflectance usually decreases while SWIR reflectance increases, which makes the dNBR index a valuable tool for evaluating changes in soil and vegetation following a fire (Van Gerrevink & Veraverbeke, 2021).

Topography

Post-fire vegetation regrowth can also be influenced by aspect and slope, which can be obtained from a digital elevation model (DEM). North-facing slopes generally have better moisture conditions for supporting vegetation regrowth due to receiving less solar radiation and having lower evapotranspiration rates, while south-facing slopes experience more solar radiation and have higher evapotranspiration rates (Fox et al., 2008). Steeper slopes can also have a negative impact on post-fire vegetation regrowth (Viana-Soto et al., 2017).

Quantifying Vegetation Regrowth

NDVI, which is commonly used to assess vegetation, is calculated using the NIR and red (R) spectral bands (Huang et al., 2021). As mentioned earlier, higher NIR values indicate healthier vegetation, while unhealthy vegetation reflects more red light, making the difference between NIR and R spectral bands a reliable indicator of vegetation health (*LP DAAC - Vegetation*, n.d.). Several studies have used NDVI to monitor post-fire vegetation (Petropoulos et al., 2014), and this study also employs it as a measure of vegetation regrowth.

Data Sources and Preprocessing

All data were processed, analyzed, and visualized using open-source Python packages in a Jupyter Notebook (v6.5.3) except for land cover and fire boundaries. The Jupyter Notebook is available on GitHub. A new environment was created for the study using Python version 3.11.2. Installing the necessary Python packages required trial and error regarding the installation order to install all packages with their required dependencies and versions. Ultimately, installing *GDAL* first allowed all packages to be installed correctly.

The land cover data and fire perimeters were processed and visualized using QGIS 3.28.5. All data were reprojected to NAD 83 UTM Zone 10N for processing and analysis. They study area map was made using QGIS. The data processing and analysis workflow can be seen in Figure 2. Additionally, QGIS was used to verify pixel alignment and clipping of the rasters produced using the Jupyter Notebook.

A list of all the Python packages used and their versions is in Appendix A. The primary Python packages used for raster processing and geospatial analyses were *NumPy*, *rasterio*, *rioxarray*, and *xarray*. *NumPy* creates and performs operations on multidimensional arrays. It was mainly

used in part of clipping multiband rasters using a single band raster and getting the raster data ready for statistical analysis.

Before *rasterio*, *GDAL* was the only option for raster processing with Python (Gillies, 2023). When opening a raster with `rasterio.open()`, a `DatasetReader` or `DatasetWriter` object is created. The object can then be read as a 2-dimensional `numpy.array` using `read(1)`, where '1' is the band number. This method was used to iteratively open, read, and process a multiband raster. The object can also be used to write a raster using `write()` or `write_band()`. When writing a raster, a raster is opened in write mode with the metadata as an argument to the function, and the `DatasetReader` or `DatasetWriter` object is read and written to the opened raster. This method was used to iteratively write processed raster bands to a new multiband raster.

When working with single band raster, *rioaxxary* was a more efficient way to open rasters because it opens and reads rasters in one step as an `xarray.DataArray` object using `rioxarray.open_rasterio()`. As is evident by the name, `open_rasterio()` was adopted from *rasterio* (*Rioxarray README — Rioxarray 0.14.0 Documentation*, n.d.). The `xarray.DataArray` object is similar to a `numpy.array` with the key difference of also storing information about the array, such as spatial data of raster (*Overview: Why Xarray?*, n.d.). Since the object is like a `numpy.array`, rasters opened using *rioxarray* can be processed using *rasterio*. Additionally, basic math calculations can be performed on `xarray.DataArray` objects without transformation. The `xarray.DataArray` objects can also be converted, and therefore saved, as a raster using `rio.to_raster()`. Using *rioxarray* to save rasters is much simpler than using *rasterio* because the metadata is already part of the `xarray.DataArray`,

and the raster is simply saved instead of needing to open a raster to write to it. This method was also used to save a multiband raster.

Throughout the analysis, different methods were used to perform the same or similar operations, such as using both *rasterio* and *rioxarray* to save multiband rasters. This was done for two reasons. The first reason was to implement the different methods available with the intention of learning which method best. The second reason is that even though a method worked to perform a particular operation, it didn't always work when performing an almost identical operation.

Land Cover

The National Land Cover Database (NLCD) is a comprehensive database that covers the entire United States and Puerto Rico, which is updated every five years at a minimum (*National Land Cover Database | U.S. Geological Survey*, 2020). Land cover data with a 30-meter resolution were obtained from the Multi-Resolution Land Characteristics Consortium website for the years 2001, 2006, 2011, 2016, and 2019 (*Data | Multi-Resolution Land Characteristics (MRLC) Consortium*, n.d.). The land cover data from 2001 were used to identify an appropriate study area, while the data from the subsequent years were reprojected and clipped to the study area without co-registration, as they were only used for visual identification of the predominant land cover types within the study area.

Fire Perimeters

The study area was chosen by selecting fire perimeters data from the CAL FIRE Fire and Resource Assessment Program, which included fires that occurred in Northern California from 2003 to 2008 with a burned area of 5,000 acres or more (California Department of Forestry and Fire Protection [CAL FIRE], n.d.). The land cover inside the fire perimeters was visually

analyzed using the 2001 NLCD to identify locations with mostly evergreen forest in mountainous areas. The Cold Fire was identified as a suitable study area and the fire perimeter was exported as a shapefile. A shapefile of the study area with a 300-meter buffer was also created.

Multispectral Imagery

The Landsat Collection 2 Analysis Ready Data (ARD) undergoes a rigorous and consistent processing method, ensuring its suitability for monitoring and evaluating landscape changes (*Landsat Collection 2 U.S. Analysis Ready Data | U.S. Geological Survey*, 2019). The raster data (listed in Table 1) with 30-meter resolution were obtained from the US Geological Survey (USGS) Earth Explorer, and efforts were made to acquire imagery from the same season to minimize seasonal variations (Ireland & Petropoulos, 2015). However, factors such as cloud cover and snowpack were also taken into account. The use of ARD greatly reduced preprocessing time as data from three different Landsat satellites were utilized. Data from Landsat 7 for the year 2012 were not included due to data loss caused by a malfunction of the satellite.

The Landsat data were provided as separate bands. The required bands for this study were the R and NIR bands for all years to calculate NDVI, bands 3 and 4 for Landsat 5, and bands 4 and 5 for Landsat 8 and 9. Additionally, the SWIR band, Landsat 5 band 7, was also needed for the year of the fire to calculate NBR and dNBR. To reduce processing time, only the necessary bands were extracted from each Landsat dataset. The shapefile of the Cold Fire perimeter was opened with *geopandas*. The extracted bands were then reprojected and clipped to the geometry

of the study area using *rioxarray*, stacked using *xarray* to create a multiband raster, and exported using *rioxarray*.

Collection Dates		
Landsat 5	**Landsat 8**	**Landsat 9**
June 6, 2008	June 28, 2013	June 29, 2022
Sept 9, 2008	June 22, 2014	
June 24, 2009	June 25, 2015	
July 6, 2010	June 20, 2016	
July 16, 2011	June 23, 2017	
	June 26, 2018	
	June 23, 2019	
	July 1, 2020	
	June 18, 2021	

Table 1 - Landsat satellites and data collection dates.

Pre- and post-fire Landsat rasters were opened using *rioxarray*. NBR (Equation 1) and dNBR (Equation 2) were calculated using basic Python math operations.

$$NBR = \frac{(NIR - SWIR)}{(NIR - SWIR)} \quad (1)$$

$$dNBR = NBR_{pre} - NBR_{post} \quad (2)$$

All the Landsat multiband rasters were opened using *rioxarray*, and NDVI (Figure 3) was calculated for each year using basic Python math operations (Equation 3). All the single band NDVI rasters were stacked in chronological order and exported as one multiband raster using *rasterio*.

$$NDVI = \frac{(NIR-R)}{(NIR+R)} \quad (3)$$

Digital Elevation Model Products

Shuttle Radar Topography Mission data were also obtained from the USGS Earth Explorer to use as the DEM. The DEM was void-filled with a 1 arc-second resolution (*USGS EROS Archive - Digital Elevation - Shuttle Radar Topography Mission (SRTM) Void Filled | U.S. Geological Survey*, 2018). Because the Landsat and DEM data had different pixel sizes, the DEM was reprojected and co-registered to match the Landsat rasters. The shapefile of the Cold Fire perimeter with a 300-meter buffer was opened using *geopandas*. One Landsat raster was clipped using *rasterio* to use for the co-registration. Since edge pixels are not included when calculating aspect and slope, 300 meters was a more than sufficient buffer to ensure all pixels within the study area boundary would be calculated. The DEM was opened and reprojected using bilinear interpolation with *rioxarray*. Co-registration was performed using *rasterio*, and the DEM was clipped to the extent of the Landsat raster and not the geometry during the co-registration process.

After co-registration, aspect and slope were calculated using the DEM using *GDAL*. The intent was to use the GDAL Python API function `DEMProcessing()` for the aspect and slope calculations; however, the results were grossly inaccurate. Instead, the GDAL shell command was executed using the Python `os.system()` function. An attempt was made to use *RichDEM*, but the save function, `SaveGDAL()`, did not work. The aspect raster contained three NoData pixels in the middle of the raster. The values for the NoData pixels were interpolated using *NumPy* and `scipy.interpolate.griddata`. The aspect and slope rasters were clipped to the study area using *rioxarray*. Although the slope raster was clipped using the same method as

other rasters, unlike the other clipped rasters, the values outside the clipped area were -9999 instead of NaN. To perform the linear regression, the values had to be NaN, so a mask was applied using *xarray*.

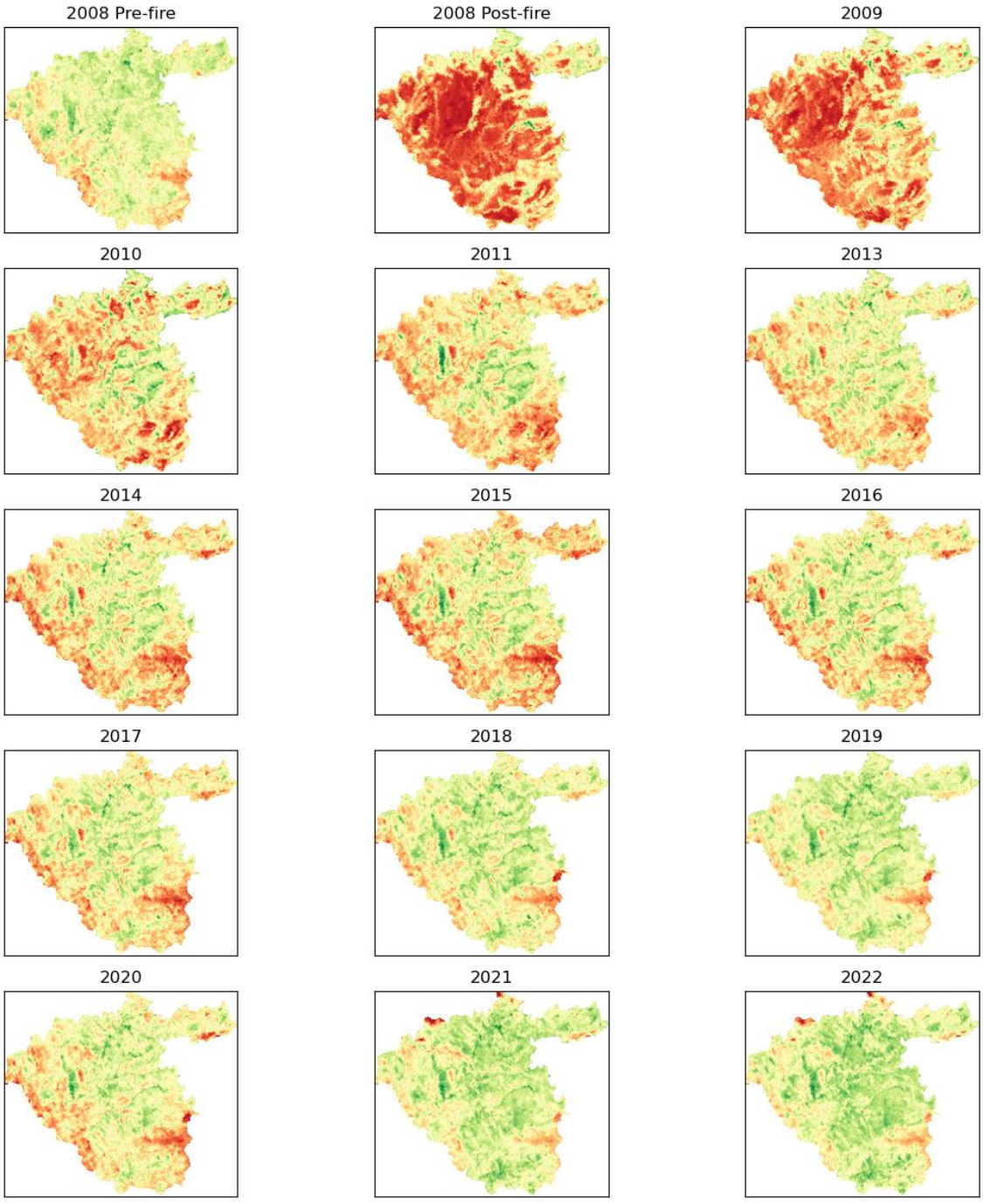

Figure 3 - NDVI pre- and post-fire. Lower values are red and higher values are green.

Classes

To compare the relationship between vegetation regrowth and topography, as well as vegetation regrowth and burn severity using a linear regression, aspect, slope, and dNBR needed to be classified with an individual raster for each class. The classifications were all performed by opening the appropriate raster using *rioxarray*, masking all non-class values with *xarray*, and saving the resulting class raster with *rioxarray* (Figure 5).

Burn Severity Level	**dNBR Range**
Enhanced Regrowth, low (post-fire)	-0.250 to -0.101
Unburned	-0.100 to +0.99
Low Severity	+1.00 to +0.269
Moderate-low Severity	+0.270 to +0.439
Moderate-high Severity	+0.440 to +0.659

Table 2 - Burn severity levels based on dNBR. Note, only severity levels applicable to the study area are shown.

Burn severity levels based on dNBR proposed by the USGS (Keeley, 2009) were used to classify the study area (Table 2). The dNBR for the study area ranged from approximately -0.144 to 0.483. Since the Enhanced Regrowth burn severity area was so small, it was combined with Unburned (Figure 4). For the same reason, Moderate-high Severity was combined with Moderate-low Severity as a Moderate Severity class.

Aspect was then classified into north-facing slopes, north and northeast aspects, and south-facing slopes, south and southwest aspects based on Meng et al. (2015). Slope was classified into three classes (Table 3) based on slope classes in the U.S. Department of Agriculture (USDA) Soil Survey Manual (Soil Science Division Staff, 2017).

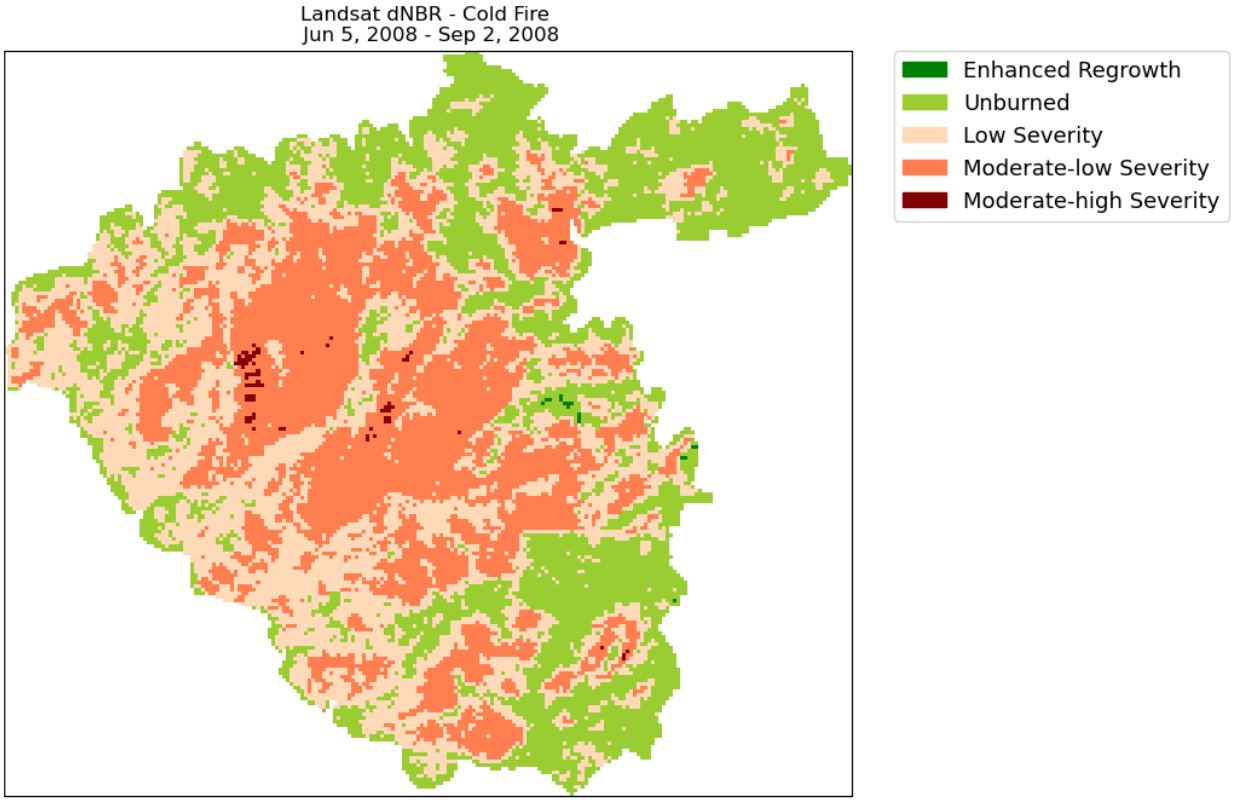

Figure 4 - Burn severity classes of the Cold Fire based on dNBR.

Slopes	Range
Mild	0 - 8%
Moderate	8 - 20%
Steep	> 20%

Table 3 - Slope classes based on USDA Soil Survey Manual.

Post-fire Vegetation Regrowth Analysis

Numerous studies have investigated vegetation regrowth after fires using various techniques. The following examples are not exhaustive but provide a snapshot of different methods used. For instance, Casady et al. (2010) employed regression trees to predict post-fire vegetation based on

burn severity, soil, and vegetation. Meng et al. (2015) used ordinary least squares regression to model post-fire vegetation recovery, taking into account precipitation, temperature, fire severity, and topographic factors. Viana-Soto et al. (2017) utilized both ordinary least squares and geographic weight regression to compare results. Tonbul et al. (2016) conducted a multitemporal analysis of NDVI and SAVI, computing statistics for each index at different stages after the fire. Bright et al. (2019) employed random forest modeling to examine the relationship between post-fire NBR recovery, climate, and topography. Finally, Petropoulos et al. (2014) compared post- and pre-fire NDVI rates of vegetation regrowth using linear regression. Similarly, the present study used linear regression to compare pre- and post-fire NDVI.

To compare the relationship between vegetation regrowth and topography and burn severity using a linear regression, the NDVI raster stack was clipped with each class raster using *rasterio* and *NumPy*. This resulted in eight different clipped NDVI raster stacks, three for burn severity, three for slope, and two for aspect. After each stack was clipped, the shape of the raster was verified to be the same shape as the class raster.

The multiband NDVI raster was opened using *GDAL*, read as an array, and converted to a `numpy.array`. The array was flattened, and all NaN values were removed. A linear regression was performed for each year post-fire for each class, as well as the entire study area using `scipy.stats.linregress`. The post-fire NDVI was the dependent variable, and the pre-fire NDVI was the independent variable. The statistics from the linear regression were stored in a `pandas.DataFrame` and exported as a *csv* file. The R-squared for each year post-fire was plotted using *matplotlib* to conduct a visual analysis of the vegetation regrowth.

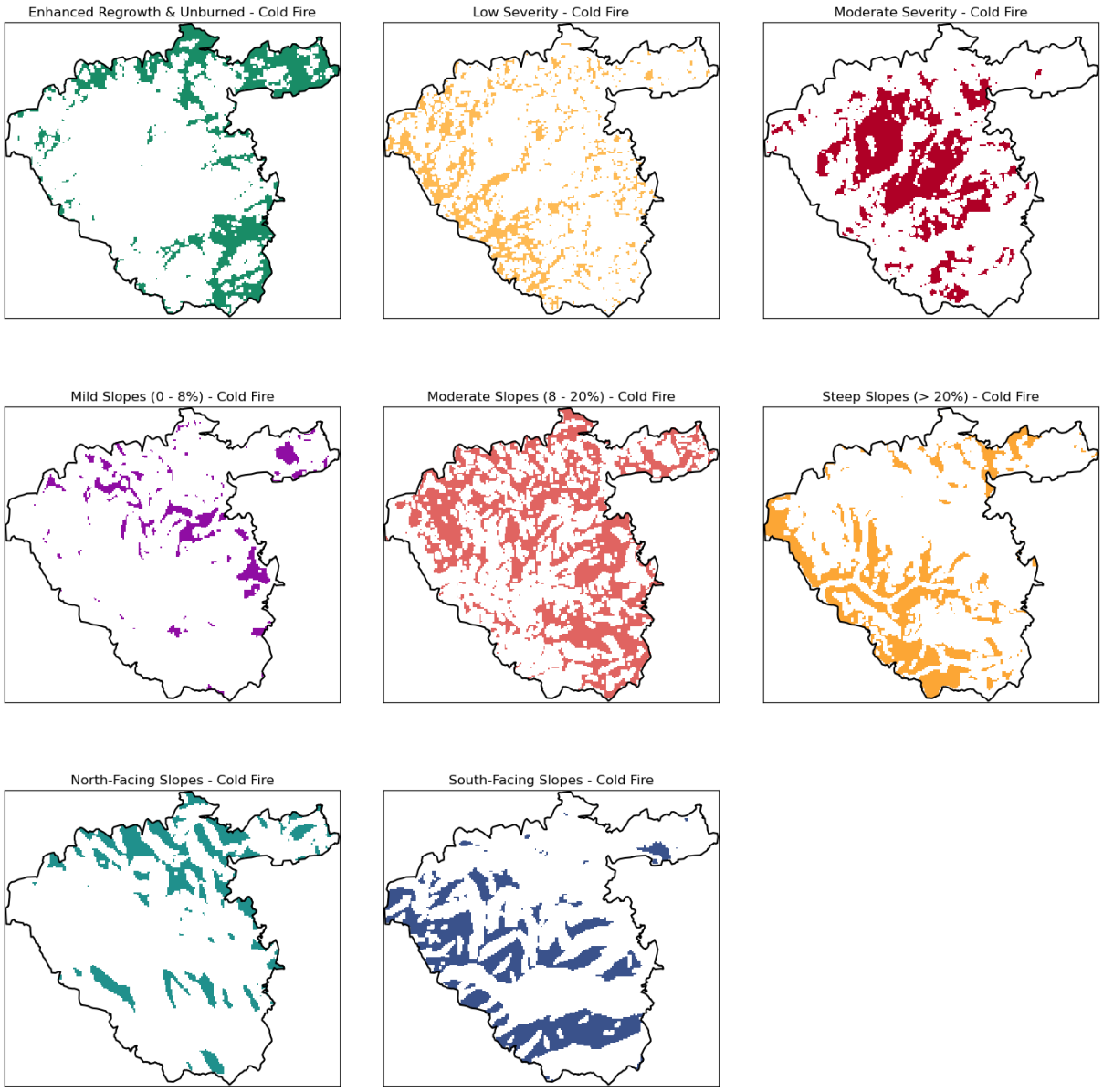

Figure 5 - dNBR-derived classes for burn severity level and DEM-derived classes for slope and aspect.

3. Results

A visual comparison of NDVI over the study period shows the vegetation damage caused by the fire, and the subsequent regrowth after the fire. Vegetation regrowth appears to mostly increase over the years post-fire, except for 2020. All plots of R-squared can be seen in Figure 6.

In the linear regression analysis, pre-fire NDVI was used as the independent variable and post-fire NDVI as the dependent variable. Therefore, higher R-squared value indicates that post-fire NDVI is closer to pre-fire NDVI. The R-squared values for the entire study area indicates that vegetation regrowth was minimal in 2009, the first year after the fire. However, vegetation regrowth increased in 2010 and 2011. As no high-quality Landsat ARD data were available for 2012, it is unclear if vegetation regrowth continued to increase at the previous rate that year or if it started to slow down like subsequent years. From 2013 to 2020, vegetation regrowth slowed down but remained relatively steady. However, in 2021, vegetation regrowth decreased significantly, and it was even lower in 2022.

The R-squared plots for topography-related factors were similar to that of the entire study area. The R-squared plot for Moderate Severity burn level was also similar to that of the entire study area. However, the vegetation regrowth for Unburned and Low Severity burn classes was notably different. In both classes, vegetation regrowth declined in 2009 and 2010. From 2011 to 2022, vegetation regrowth for the Low Severity burn class was similar to that of the entire study area. For the Unburned burn class, vegetation regrowth was relatively constant until 2019, with some minor ups and downs. However, unlike the Low and Moderate Severity burn classes, vegetation regrowth in the Unburned area started to decrease in 2019, and from 2020 to 2022, it declined even further.

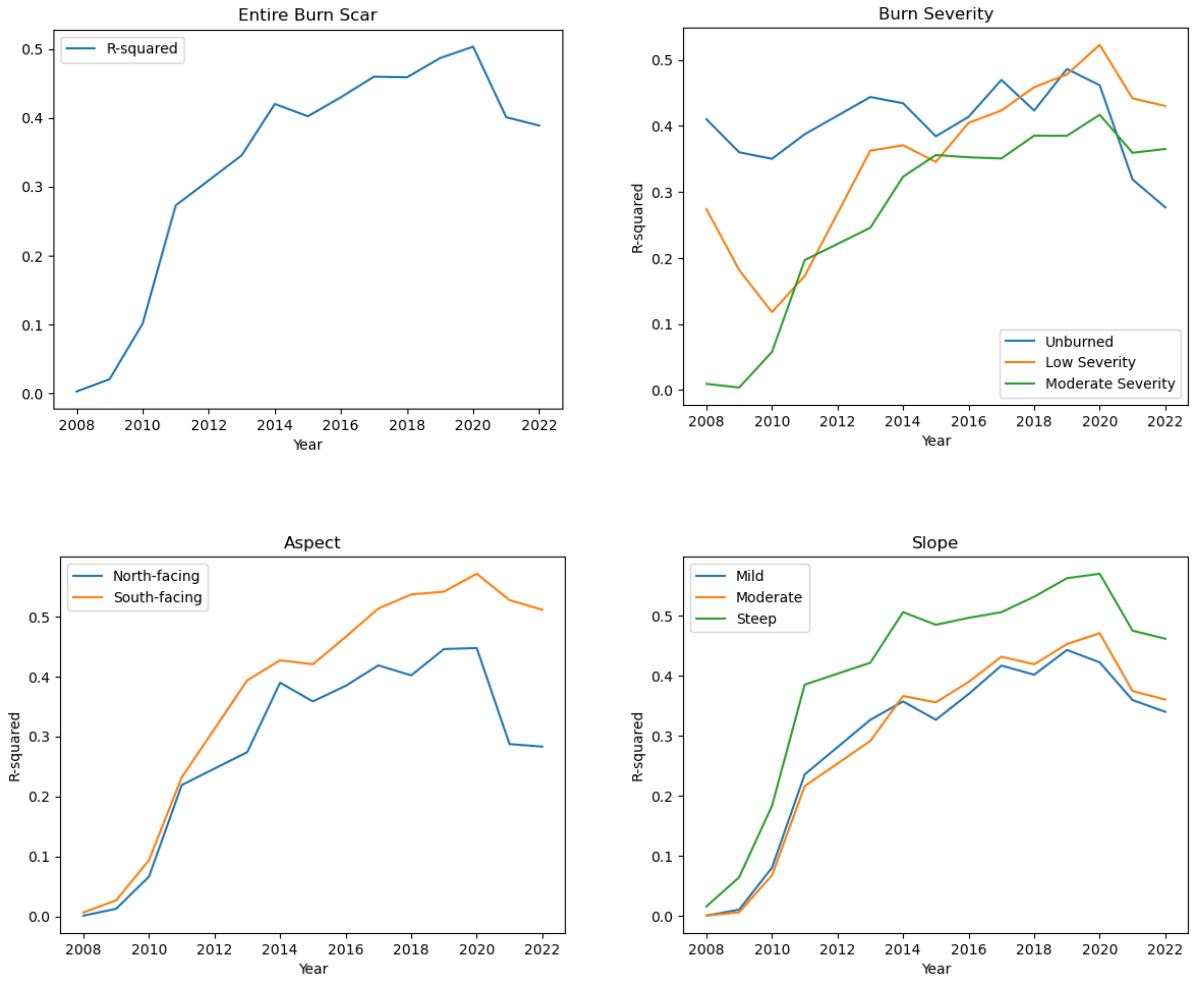

Figure 6 - R-squared results from linear regression.

4. Discussion

Based on the findings of this study, there is considerable spatial diversity in the recovery of vegetation after a fire. Moreover, the results indicate that vegetation regrowth following a fire is a gradual process, with the vegetation coverage in the burn area not reaching pre-fire levels even after 14 years. One plausible explanation for this could be vegetation type conversion, as shown

in Figure 7. Nevertheless, to validate this hypothesis, it would be necessary to conduct on-site verification.

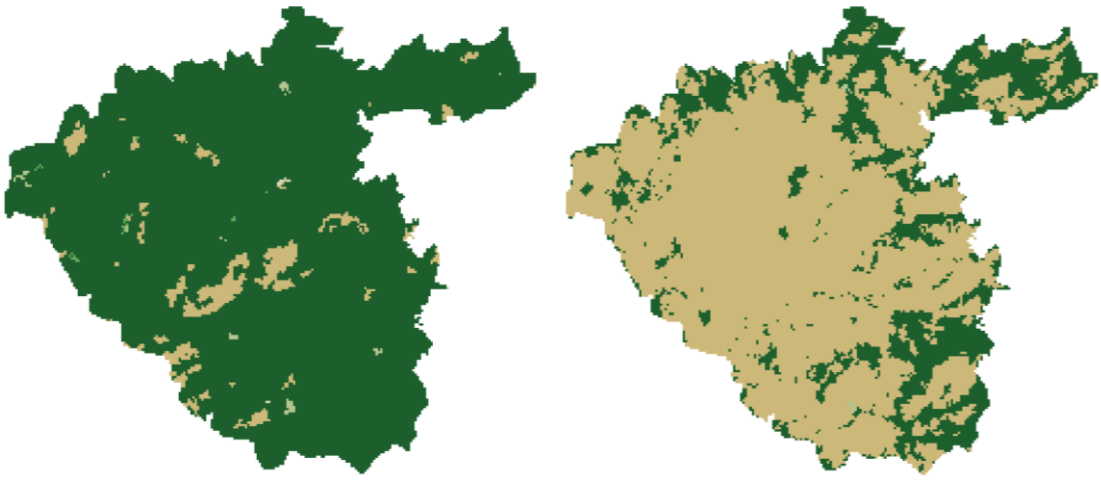

Figure 7 - According to the NLCD, pre-fire vegetation in 2006 (left) was mostly evergreen forest (dark green) with some shrub/scrub (tan). Post-fire vegetation in 2019 (right) consisted mostly of shrub/scrub with some everything forest; however, much of the post-fire evergreen forest consists of vegetation that survived the fire.

Although the Cold Fire did not result in any high severity burn areas, regions with lower burn severity demonstrated higher regrowth, which is consistent with the findings of other studies (Petropoulos et al., 2014; Crotteau et al., 2013). The degree of vegetation loss caused by a fire is illustrated by the dNBR, but comparing the burn severity of areas with different pre-fire vegetation levels may not yield an accurate depiction. This is because locations with more pre-fire vegetation may have higher dNBR values, even if they experience a comparable level of burn severity as areas with lower pre-fire vegetation (Casady et al., 2010).

Like other studies (Meng et al., 2015; Bright et al., 2019), vegetation regrowth was higher the first few years after the fire starting one-year post-fire. Unlike the studies by Petropoulos et al.

(2014) and Fox et al. (2008) which found vegetation regrowth to be higher on north-facing slopes, south-facing slopes in the Cold Fire burn scar had a higher regrowth rate after 2011. The results also disproved the hypothesis of lower vegetation regrowth on steeper slopes.

5. Conclusion

The use of FOSS for GIS for this post-fire vegetation regrowth analysis was effective, albeit challenging due to the programming involved. Due to my inexperience with geospatial analysis using Python, many days were dedicated to the programming for this analysis. Most of the time spent on this study involved researching how to obtain the desired results using the various Python libraries and debugging code. The analysis would have taken less than a day using proprietary software, like ArcGIS, and not much longer than that using an unfamiliar FOSS, like QGIS.

As for the post-fire vegetation regrowth analysis itself, the unexpected results of increased growth on steeper slopes and south-facing slopes warrant investigation in a future study. Slope shape could be used instead of slope angle like in the study by Bright et al. (2019). Additionally, the relative dNBR which normalizes dNBR for variations in pre-fire vegetation could be used instead of dNBR for burn severity classification (Cai & Wang, 2020). To further analyze post-fire vegetation regrowth, different analysis methods could be used to compare results. The study could also be expanded to include many burn scars to analyze the differences in vegetation regrowth across different landscapes, and climate factors could be included.

References

After Fire: Toolkit for the Southwest. (n.d.). US Forest Service Research and Development. Retrieved April 29, 2023, from https://www.fs.usda.gov/research/rmrs/products/dataandtools/tools/after-fire-toolkit-southwest

Arianoutsou, M., Koukoulas, S., & Kazanis, D. (2011). Evaluating Post-Fire Forest Resilience Using GIS and Multi-Criteria Analysis: An Example from Cape Sounion National Park, Greece. *Environmental Management*, *47*(3), 384–397. https://doi.org/10.1007/s00267-011-9614-7

Bright, B. C., Hudak, A. T., Kennedy, R. T., Braaten, J., & Khalyani, A. H. (2019). Examining post-fire vegetation recovery with Landsat time series analysis in three western North American forest types. *Fire Ecology*, *15*(1). https://doi.org/10.1186/s42408-018-0021-9

Cai, L., & Wang, M. (2020). Is the RdNBR a better estimator of wildfire burn severity than the dNBR? A discussion and case study in southeast China. *Geocarto International*, *37*(3), 758–772. https://doi.org/10.1080/10106049.2020.1737973

California Department of Forestry and Fire Protection [CAL FIRE]. (n.d.). *Fire Perimeters | CAL FIRE*. Retrieved April 8, 2023, from https://www.fire.ca.gov/what-we-do/fire-resource-assessment-program/fire-perimeters

Casady, G. M., Van Leeuwen, W. B., & Marsh, S. (2010). Evaluating Post-wildfire Vegetation Regeneration as a Response to Multiple Environmental Determinants. *Environmental Modeling & Assessment*, *15*(5), 295–307. https://doi.org/10.1007/s10666-009-9210-x

Coetzee, S., Ivánová, I., Mitasova, H., & Brovelli, M. A. (2020). Open Geospatial Software and Data: A Review of the Current State and A Perspective into the Future. *ISPRS International Journal of Geo-information*, *9*(2), 90. https://doi.org/10.3390/ijgi9020090

Crotteau, J. S., Varner, J. M., & Ritchie, M. W. (2013). Post-fire regeneration across a fire severity gradient in the southern Cascades. *Forest Ecology and Management*, *287*, 103–112. https://doi.org/10.1016/j.foreco.2012.09.022

Data | Multi-Resolution Land Characteristics (MRLC) Consortium. (n.d.). Retrieved April 20, 2023, from https://www.mrlc.gov/data

Duarte, L., Marques, J. S., & Teodoro, A. C. (2019). An Open Source GIS-Based Application for the Assessment of Groundwater Vulnerability to Pollution. *Environments*, *6*(7), 86. https://doi.org/10.3390/environments6070086

Ecoregions | US EPA. (2022, July 5). US EPA. https://www.epa.gov/eco-research/ecoregions

Flenniken, J. M., Stuglik, S., & Iannone, B. V. (2020). Quantum GIS (QGIS): An introduction to a free alternative to more costly GIS platforms. *EDIS*, *2020*(2), 7. https://doi.org/10.32473/edis-fr428-2020

Fox, D., Maselli, F., & Carrega, P. (2008). Using SPOT images and field sampling to map burn severity and vegetation factors affecting post forest fire erosion risk. *Catena*, *75*(3), 326–335. https://doi.org/10.1016/j.catena.2008.08.001

Gillies, S. (2023). rasterio Documentation. *Map Box*.

Guiterman, C. H., Gregg, R. M., Marshall, L. J., Beckmann, J. J., Van Mantgem, P. J., Falk, D. A., Keeley, J. E., Caprio, A. C., Coop, J. D., Fornwalt, P. J., Haffey, C., Hagmann, R. K., Jackson, S. P., Lynch, A. M., Margolis, E. Q., Marks, C. R., Meyer, M. H., Safford, H. D., Syphard, A. D., . . . Stevens, J. T. (2022). Vegetation type conversion in the US Southwest: frontline observations and management responses. *Fire Ecology*, *18*(1). https://doi.org/10.1186/s42408-022-00131-w

Harvey, B. H., Donato, D. C., & Turner, M. G. (2016). High and dry: post-fire tree seedling establishment in subalpine forests decreases with post-fire drought and large stand-replacing burn patches. *Global Ecology and Biogeography*, *25*(6), 655–669. https://doi.org/10.1111/geb.12443

Holzman, M., Rivas, R., & Bayala, M. I. (2021). Relationship between TIR and NIR-SWIR as Indicator of Vegetation Water Availability. *Remote Sensing*, *13*(17), 3371. https://doi.org/10.3390/rs13173371

Huang, S., Tang, L., Hupy, J. P., Wang, Y., & Shao, G. (2021). A commentary review on the use of normalized difference vegetation index (NDVI) in the era of popular remote sensing. *Journal of Forestry Research*, *32*(1), 1–6. https://doi.org/10.1007/s11676-020-01155-1

Ireland, G., & Petropoulos, G. P. (2015). Exploring the relationships between post-fire vegetation regeneration dynamics, topography and burn severity: A case study from the Montane Cordillera Ecozones of Western Canada. *Applied Geography*, *56*, 232–248. https://doi.org/10.1016/j.apgeog.2014.11.016

Johnson, E., & Gutsell, S. L. (1993). Heat budget and fire behaviour associated with the opening of serotinous cones in two*Pinus*species. *Journal of Vegetation Science*, *4*(6), 745–750. https://doi.org/10.2307/3235610

Johnstone, J. F., & Chapin, F. S. (2006). Effects of Soil Burn Severity on Post-Fire Tree Recruitment in Boreal Forest. *Ecosystems*, *9*(1), 14–31. https://doi.org/10.1007/s10021-004-0042-x

Keeley, J. E. (2009). Fire intensity, fire severity and burn severity: a brief review and suggested usage. *International Journal of Wildland Fire*, *18*(1), 116. https://doi.org/10.1071/wf07049

Knevels, R., Petschko, H., Leopold, P. L., & Brenning, A. (2019). Geographic Object-Based Image Analysis for Automated Landslide Detection Using Open Source GIS Software. *ISPRS International Journal of Geo-information*, *8*(12), 551. https://doi.org/10.3390/ijgi8120551

Landsat Collection 2 U.S. Analysis Ready Data | U.S. Geological Survey. (2019, November 14). https://www.usgs.gov/landsat-missions/landsat-collection-2-us-analysis-ready-data

LP DAAC - Vegetation. (n.d.). Retrieved May 1, 2023, from https://lpdaac.usgs.gov/data/get-started-data/workflow-examples/

Lutes, D. C., Keane, R. E., Caratti, J. F., Key, C. H., Benson, N. C., Sutherland, S., & Gangi, L. J. (2006). *FIREMON: Fire effects monitoring and inventory system*. https://doi.org/10.2737/rmrs-gtr-164

Mangiameli, M., Mussumeci, G., & Cappello, A. (2021). Forest Fire Spreading Using Free and Open-Source GIS Technologies. *Geomatics*, *1*(1), 50–64. https://doi.org/10.3390/geomatics1010005

Mattivi, P., Franci, F., Lambertini, A., & Bitelli, G. (2019). TWI computation: a comparison of different open source GISs. *Open Geospatial Data, Software and Standards*, *4*(1). https://doi.org/10.1186/s40965-019-0066-y

Maurya, S. P., Ohri, A., & Mishra, S. (2015). Open Source GIS: A Review. *ResearchGate*. https://www.researchgate.net/publication/282858368

Meng, R., Dennison, P. E., Huang, C., Moritz, M. A., & D'Antonio, C. M. (2015). Effects of fire severity and post-fire climate on short-term vegetation recovery of mixed-conifer and red fir forests in the Sierra Nevada Mountains of California. *Remote Sensing of Environment, 171*, 311–325. https://doi.org/10.1016/j.rse.2015.10.024

Mitri, G., & Gitas, I. Z. (2013). Mapping post-fire forest regeneration and vegetation recovery using a combination of very high spatial resolution and hyperspectral satellite imagery. *International Journal of Applied Earth Observation and Geoinformation, 20*, 60–66. https://doi.org/10.1016/j.jag.2011.09.001

Muenchow, J., Schäfer, S., & Krüger, E. (2019). Reviewing qualitative GIS research—Toward a wider usage of open-source GIS and reproducible research practices. *Geography Compass, 13*(6). https://doi.org/10.1111/gec3.12441

National Land Cover Database | U.S. Geological Survey. (2020, May 26). https://www.usgs.gov/centers/eros/science/national-land-cover-database#overview

NOAA's National Weather Service. (n.d.). *Climate*. Retrieved May 1, 2023, from https://www.weather.gov/wrh/Climate?wfo=sto

OSGeo Description - OSGeo. (n.d.). https://wiki.osgeo.org/wiki/OSGeo_Description

Overview: Why xarray? (n.d.). Xarray. https://docs.xarray.dev/en/stable/getting-started-guide/why-xarray.html

Petropoulos, G. P., Griffiths, H., & Kalivas, D. (2014). Quantifying spatial and temporal vegetation recovery dynamics following a wildfire event in a Mediterranean landscape using EO data and GIS. *Applied Geography*, *50*, 120–131. https://doi.org/10.1016/j.apgeog.2014.02.006

Reflected Near-Infrared Waves | Science Mission Directorate. (n.d.). Retrieved April 30, 2023, from https://science.nasa.gov/ems/08_nearinfraredwaves

rioxarray README — rioxarray 0.14.0 documentation. (n.d.). https://corteva.github.io/rioxarray/stable/readme.html

Savage, M., Mast, J. N., & Feddema, J. (2013). Double whammy: high-severity fire and drought in ponderosa pine forests of the Southwest. *Canadian Journal of Forest Research*, *43*(6), 570–583. https://doi.org/10.1139/cjfr-2012-0404

Soil Science Division Staff. (2017). *Soil Survey Manual: Vol. USDA Handbook 18* (C. Ditzler, K. Scheffe, & H. C. Monger, Eds.). Government Printing Office.

Strand, E. K., Satterberg, K. L., Hudak, A. T., Byrne, J. H., Khalyani, A. H., & Smith, A. M. S. (2019). Does burn severity affect plant community diversity and composition in mixed conifer forests of the United States Intermountain West one decade post fire? *Fire Ecology*, *15*(1). https://doi.org/10.1186/s42408-019-0038-8

Tonbul, H., Kavzoglu, T., & Kaya, S. (2016). ASSESSMENT OF FIRE SEVERITY AND POST-FIRE REGENERATION BASED ON TOPOGRAPHICAL FEATURES USING MULTITEMPORAL LANDSAT IMAGERY: A CASE STUDY in MERSIN, TURKEY. *The International Archives of the Photogrammetry, Remote Sensing and Spatial Information Sciences*, *XLI-B8*, 763–769. https://doi.org/10.5194/isprsarchives-xli-b8-763-2016

Urza, A. K., & Sibold, J. S. (2017). Climate and seed availability initiate alternate post-fire trajectories in a lower subalpine forest. *Journal of Vegetation Science*, *28*(1), 43–56. https://doi.org/10.1111/jvs.12465

USGS EROS Archive - Digital Elevation - Shuttle Radar Topography Mission (SRTM) Void Filled | U.S. Geological Survey. (2018, July 30). https://www.usgs.gov/centers/eros/science/usgs-eros-archive-digital-elevation-shuttle-radar-topography-mission-srtm-void?qt-science_center_objects=0#qt-science_center_objects

Van Gerrevink, M. J., & Veraverbeke, S. (2021). Evaluating the Near and Mid Infrared Bi-Spectral Space for Assessing Fire Severity and Comparison with the Differenced Normalized Burn Ratio. *Remote Sensing*, *13*(4), 695. https://doi.org/10.3390/rs13040695

Viana-Soto, A., Aguado, I., & Martínez, S. (2017). Assessment of Post-Fire Vegetation Recovery Using Fire Severity and Geographical Data in the Mediterranean Region (Spain). *Environments*, *4*(4), 90. https://doi.org/10.3390/environments4040090

Welch, K. D., Safford, H. D., & Young, T. P. (2016). Predicting conifer establishment post wildfire in mixed conifer forests of the North American Mediterranean-climate zone. *Ecosphere*, *7*(12). https://doi.org/10.1002/ecs2.1609

Wittenberg, L. (2021). Post-fire Soil Erosion – The Mediterranean Perception. In *Managing forest ecosystems*. Springer Nature (Netherlands). https://doi.org/10.1007/978-3-030-63625-8_23

Appendix A: Python packages used for data processing and analysis

pandas 1.5.3

geopandas 0.12.2

NumPy 1.24.2

xarray 2023.3.0

rioxarray 0.14.0

earthpy 0.9.4

rasterio 1.3.6

matplotlib 3.7.1

GDAL 3.6.3

scipy 1.10.1

shapely 2.0.1